View metadata, citation and similar papers at core.ac.uk

brought to you by CORE

provided by University of Birmingham Research Portal

UNIVERSITY OF BIRMINGHAM

Research at Birmingham

Investigation of the problems with using gas adsorption to probe catalyst pore structure evolution during coking

Gopinathan, N.; Greaves, M.; Wood, Joseph; Rigby, S.P.

DOI:
10.1016/j.jcis.2012.10.025

License:
None: All rights reserved

Document Version
Early version, also known as pre-print

Citation for published version (Harvard):
Gopinathan, N, Greaves, M, Wood, J & Rigby, SP 2012, 'Investigation of the problems with using gas adsorption to probe catalyst pore structure evolution during coking', Journal of Colloid and Interface Science, pp. 234–240. https://doi.org/10.1016/j.jcis.2012.10.025

Link to publication on Research at Birmingham portal

Publisher Rights Statement:

NOTICE: this is the author's version of a work that was accepted for publication in Journal of Colloid and Interface Science. Changes resulting from the publishing process, such as peer review, editing, corrections, structural formatting, and other quality control mechanisms may not be reflected in this document. Changes may have been made to this work since it was submitted for publication. A definitive version was subsequently published in Journal of Colloid and Interface Science Volume 393, 1 March 2013, Pages 234–240 http://dx.doi.org/10.1016/j.jcis.2012.10.025

General rights
Unless a licence is specified above, all rights (including copyright and moral rights) in this document are retained by the authors and/or the copyright holders. The express permission of the copyright holder must be obtained for any use of this material other than for purposes permitted by law.

• Users may freely distribute the URL that is used to identify this publication.
• Users may download and/or print one copy of the publication from the University of Birmingham research portal for the purpose of private study or non-commercial research.
• User may use extracts from the document in line with the concept of 'fair dealing' under the Copyright, Designs and Patents Act 1988 (?)
• Users may not further distribute the material nor use it for the purposes of commercial gain.

Where a licence is displayed above, please note the terms and conditions of the licence govern your use of this document.

When citing, please reference the published version.

Take down policy
While the University of Birmingham exercises care and attention in making items available there are rare occasions when an item has been uploaded in error or has been deemed to be commercially or otherwise sensitive.

If you believe that this is the case for this document, please contact UBIRA@lists.bham.ac.uk providing details and we will remove access to the work immediately and investigate.

Download date: 01. Feb. 2019

The problems with using gas adsorption to track catalyst pore structure evolution during coking

Navin Gopinathan[a], Malcolm Greaves[a], John P. Lowe[b], Joseph Wood[c], Sean P. Rigby[d]*

[a]*Department of Chemical Engineering, University of Bath, Claverton Down, Bath BA2 7AY, U.K.*

[b]*Department of Chemistry, University of Bath, Claverton Down, Bath BA2 7AY, U.K.*

[c]*Centre for Formulation Engineering, Department of Chemical Engineering, School of Engineering, The University of Birmingham, Edgbaston, Birmingham B15 2TT, U.K.*

[d]*Department of Chemical and Environmental Engineering, University of Nottingham, University Park, Nottingham NG7 2RD, UK*

*Corresponding author

Telephone No.: +44 (0) 115 951 4078

Email: enzspr@exmail.nottingham.ac.uk

ABSTRACT

A common approach to try to understand the mechanism of coking in heterogeneous catalysts is to monitor the evolution of the pore structure using gas adsorption analysis of discharged pellets. However, the standard methods of analysis of gas adsorption data, to obtain pore-size distributions, make the critical assumption of thermodynamically-independent pores. This assumption neglects the possibility of co-operative adsorption phenomena. In this work the serial adsorption technique has been used to detect and assess the extent of co-operative effects in adsorption within coking catalysts. It has been shown that the conventional analysis method would lead to a flawed picture of the pore structure changes during the coking process. The serial adsorption technique thus provides a more accurate method to detect pore structure evolution during coking. A study of the kinetics of adsorption has been used to infer information about the general spatial location of the coking process within a pellet.

Keywords: adsorption; pore structure; deactivation

INTRODUCTION

The heterogeneous catalysts used in processes involving transformation of hydrocarbons are prone to deactivation by deposition of carbonaceous material, commonly known as 'coke'. The economics of these processes can be improved by extending the lifetime of the catalyst, in order to reduce the necessity for halting production for changes in catalyst charges. Studies of catalyst coking aim to understand the coking mechanism to enable the design of more resistant catalysts. In order to follow and understand catalyst coking, the evolution of the pore structure is often monitored by periodic discharge of samples that are then characterised using gas sorption. Many previous studies have monitored structural changes via changes to the shape of gas sorption isotherms [1], and/or to the BET specific surface area and pore size distribution (PSD) derived from the isotherms [2]. In most cases, the gas used for the characterisation is nitrogen, but other substances, such as water [3] or hydrocarbons [4], are also sometimes used. Mechanisms of deactivation by coking, such as pore mouth blocking, or more pervasive site coverage, are then inferred from observed changes to the surface area or pore size distribution [5]. The level of correct understanding concerning the coking process thereby derived thus relies heavily upon the accuracy of the pore size distributions obtained. However, there are a number of problems with conventional methods to determine pore size distributions from gas adsorption, which will be discussed below.

For nitrogen at 77 K, the adsorption process, in a given pore, is generally thought to consist of initial build-up of adsorbed layers on the pore walls, followed by pore-filling by capillary condensation at the particular pressure characteristic of the specific pore size, as given by the Kelvin equation. For a porous solid possessing a distribution in pore sizes, the probability density function of pore size weighted by pore volume (usually simply called the PSD) can be obtained from the nitrogen adsorption isotherm using an algorithm such as the Barrett-Joyner-Halenda method [6]. This algorithm makes the assumption that pores of different sizes are thermodynamically independent. This is equivalent to treating the individual 'pores' within an irregular, interconnected void space as if they were located within a hypothetical parallel pore bundle (i.e. a 'wine-rack' type structure). Even assuming it is possible to obtain a physically meaningful definition of a 'single pore' within an irregular, interconnected void space, this assumption neglects the possibility of interactions between neighbouring pores, or

even over much larger length-scales. Alternative methods, such as non-local density functional theory (NLDFT) [7], improve on the pore-scale physics of the phase transition but still make the same assumptions regarding thermodynamically independent pores in subsequently calculating the PSD from the adsorption isotherm.

From considerations of basic adsorption theory, involving the Kelvin equation, it is possible to deduce that cooperative pore-pore interaction phenomena will occur during adsorption [8]. Theory suggests that, for a through (open) ink-bottle pore geometry, if the radius of the two shielding pore necks is greater than half that of the intermediate pore body then all will fill at the same pressure. In this case, the pressure required is equivalent to that given by the Cohan [9] equation for a cylindrical meniscus in the pore neck. This is because once condensate has filled the pore neck, filling of the pore body may then proceed via ingress of the, now hemispherical, meniscus from the end of the pore neck. If the pore neck radius is over half that of the pore body, then the pressure for condensation within the pore body, for a hemispherical meniscus, is exceeded by the pressure required to condense in the neck with a cylindrical meniscus. This process is known as the ‘advanced adsorption’ or ‘advanced condensation’ effect. This general picture, suggested by de Boer [8], has been confirmed by grand canonical Monte-Carlo (GCMC) simulations of argon adsorption in model, unconnected silica and alumina pores possessing corrugations [9,10]. Cooperative effects during adsorption have also been observed directly by experiment, both at the pore-scale in model controlled-pore size materials, such as anodized alumina [12], and over larger macroscopic length-scales using MRI [13].

As suggested by simulation in previous work [14], the aforementioned advanced adsorption phenomena have particular, significant implications for the interpretation of gas adsorption data for samples undergoing coking reactions. For example, the above theory suggests that, if a sample were undergoing pore-mouth blocking, then, while the size of the narrow neck forming (via coke deposits) at the periphery of the pore exceeded half the size of the remaining pore body, advanced condensation would mean that it would appear that the whole pore length was being reduced in diameter, rather than just the mouth. Further, if coking was occurring on the surface of a larger pore body, located within the pellet, that was shielded by a pre-existing narrower pore neck, then, once the pore body size decreased below twice the

neck size, it would appear that the body had shrunk to the size of the neck, even if it really still remained larger. Given that simple theoretical considerations suggest that advanced adsorption phenomena should be particularly relevant to interpreting characterisation data for coking catalysts, and experiment has shown that these particular phenomena do arise in much simpler model systems, this suggests it is important to assess the significance of these effects for coking catalysts. Thus, the aim of this work is to detect, and assess the impact of, advanced adsorption effects in the structural characterisation of catalysts undergoing a coking reaction.

The most commonly used adsorbent for structural characterisation work is nitrogen. The adsorption of nitrogen within a porous solid can be monitored using scattering techniques [15], but the measured signal is necessarily averaged over a relatively large sample volume, and thus loses pore-specific information in disordered samples. Water adsorption has been proposed as an alternative adsorbent for characterisation of coked catalysts [3]. While water adsorption isotherms for many catalyst materials are Type III, indicating specific adsorption on sparse sites, in other materials, such as studied here, the isotherm shape is Type IV, similar to that typically obtained for nitrogen. The advantage of water adsorption is that it can be monitored at the pore scale using serial adsorption experiments, whereby the dry void space is first characterised by nitrogen adsorption, then a water isotherm is performed to a given relative pressure, whereupon the adsorbed water is frozen in place, and then a subsequent nitrogen adsorption experiment is conducted. This type of experiment has been used to study water sorption in silicas [16], and to probe percolation properties in templated materials [17]. In this work, serial adsorption experiments will be used to detect advanced adsorption phenomena occurring during water adsorption in fresh and coked catalysts. Previous work [18] has also demonstrated the value of a consideration of the adsorption kinetics, as well as the equilibrium isotherms, in aiding characterisation of a coking catalyst.

This paper is constructed as follows. First the experimental methods will be described. Then the results of the serial adsorption experiments will be presented and analysed. Finally, the interpretation and implications of the findings will be discussed, and some conclusions drawn.

EXPERIMENTAL

Materials

An industrial, hydroprocessing catalyst, denoted A, and its coked counterparts, denoted C1 and C2, were used for the characterisation experiments in this work. Sample A was Ketjenfine hydroprocessing catalyst-CoMo type. The composition (% w/w) of the catalyst was as follows: precipitated silica: 0-6; cobalt (II) oxide: 1-10; molybdenum (VI) oxide: < 25; phosphorus pentoxide: 0-4; aluminium oxide: balance. The as-received form of the catalyst was a blue extrudate of typical diameter ~1 mm, and typical length ~7 mm. The samples were characterised in their whole form. This material was chosen because the water adsorption isotherms show a conventional Type IV form. The BET constant, obtained from a fit of the conventional single-component BET equation to the water adsorption isotherm, for the fresh sample is 88±2. This value is in the range of BET constant values ($50<C<200$) recommend by Rouquerol *et al.* [19] to ensure that adsorption is not too loosely bound (such that the molecules are not closely packed on the surface), or too specific in nature.

Coked samples were obtained following reaction involving a model feed in the CAPRI® microreactor at the University of Birmingham [20]. The oil fed into the reactor was decane at 1 ml min^{-1}. The reaction was conducted at 425 °C and the pressure was fixed at 20 bar. The time on-stream was 60 min.

Methods

Gravimetric adsorption on fresh and coked catalyst samples was performed using a Hiden IGA-002 (Intelligent Gravimetric Analyser) system. The IGA SS316N chamber was opened and ~100 mg of the catalyst was loaded onto the sample hammock, which was hung from a microbalance. The reactor chamber was then sealed tightly and the sample was evacuated to vacuum and heated to 90 °C for an hour, followed by a more intense heat treatment at 350 °C

for four hours. This heat treatment was applied to fresh catalysts. Coked catalysts were heat treated at 150 °C for approximately twelve hours under similar vacuum conditions. After completing the heat treatment, the IGA reactor was allowed to cool to room temperature and an insulation jacket was placed around the reactor. The reactor was then immersed in a liquid nitrogen dewar, that was regularly topped-up at 3-4 hour intervals to maintain isothermal conditions.

Water vapour adsorption was done using the same system by changing the valve position and installing a supply of ~20 ml of water in a vapour reservoir. The shifting of the valve position allowed the machine to operate in the vapour mode. The vapour reservoir was cleaned and dried in an oven before adding ultrapure water (having a resistivity of 18.2 $M\Omega^{-cm}$). This water supply was then degassed. The partial saturation of the catalyst with water vapour was carried out after re-preparing the catalyst samples as above and ending the water vapour isotherm at a pressure of ~22 mbars, which corresponded to a relative pressure of ~0.7 at 298 K, rather than the saturated vapour pressure. This was achieved using the pressure control system available in the machine. At this pressure, there was sufficient capillary condensation to ensure that some of the pores in the catalyst were filled. A full water vapour isotherm performed prior to the partial water vapour adsorption experiment helped to confirm this observation.

All water vapour adsorption experiments were performed at 298 K. At this temperature, the IGA SS316N reactor was surrounded by an ethylene glycol jacket. The jacket was connected to an external chiller which could be topped with ethylene glycol and had an automated temperature control system. To ensure complete equilibrium of the process, the catalyst was maintained at relative pressure of 0.7 for approximately 12 hours. This particular partial pressure was chosen because of its relevance to coking, as will be seen below. At the end of the partial saturation, the ethylene glycol jacket was manually removed and the sample chamber was covered with an insulation jacket. A liquid nitrogen dewar half filled with liquid nitrogen was placed below the IGA reactor. The atmospheric water vapour present in the reactor was removed by outgassing at 1000 Pa min^{-1} (10 mbars min^{-1}). This low rate of degassing ensured that the atmospheric water vapour was removed. Subsequently, the remaining half of the dewar was filled with liquid nitrogen and the mass reading was allowed

to stabilise. The nitrogen isotherm for the same sample after partial saturation with water was then obtained by bringing the machine back to gas mode and performing the experiment.

Mercury porosimetry experiments were performed by using a Micromeritics Autopore III 9420 apparatus. Fresh catalyst samples were packed and sealed in a penetrometer using a light coating of vacuum grease along the lip of the penetrometer bulb. This setup was then carefully loaded into the low pressure port available in the apparatus with $\frac{1}{4}^{th}$ of its stem coated with a thin coating of silicone high vacuum grease. Then the set up was evacuated to a pressure of ~6.7×10^{-6} MPa (~50 μm Hg) in order to remove all the physisorbed water and air from the sample and the penetrometer bulb. All control of the apparatus was possible through an interface controller that was attached to a lab PC. Immediately after degassing, the apparatus performed a low pressure analysis during which pressure was increased stepwise from 0.0035 MPa up to atmospheric pressure (~0.1 MPa). Next the penetrometer assembly containing mercury was carefully removed and the silicone high vacuum grease along the stem wiped off. The assembly weight was noted. This sealed assembly was then transferred to a high pressure port after which the port was filled with a high pressure fluid up to the ledge level, and closed tightly to ensure no oil leakage. Once this setup was arranged, the high pressure analysis was initiated. This involved pressure steps from atmospheric pressure (0.1 MPa) to 413 MPa, the maximum achievable pressure of the apparatus. The equilibration time selected for analysis was 30 s, which was found to lead to fully equilibrated curves. Initial analysis was conducted by assuming a constant contact angle θ of 130°, and the mercury surface tension γ was assumed to be 0.485 Nm^{-1}. Prior to performing mercury porosimetry experiments on samples, blank runs and reference material tests using the same penetrometers and ports were performed. This helped to minimize errors related to compression and heating, and also confirm that the results obtained were representative of the material studied.

RESULTS

Mercury porosimetry

Figure 1 shows the mercury porosimetry data for a fresh sample of catalyst, obtained with an equilibration time of 30 s. The modal pore size in the intrusion curve is ~7.5 nm. The total intra-particle pore volume intruded by mercury was 0.41 ml g^{-1}. It can be seen that entrapment is nearly 100 %. This high entrapment may be an indication that mercury partially wets the surface, given that the catalyst surface contains heavy atoms, such as Co and Mo.

Gas adsorption

The nitrogen adsorption isotherms obtained for each sample before and after water adsorption are shown in Figures 2-3. Also shown in Figures 2-3 are the intermediate water adsorption isotherms. Figure 2 shows the nitrogen adsorption isotherms obtained before and after water adsorption, and the intermediate water adsorption isotherm, for a fresh sample, but with the amount adsorbed, in each case, expressed as the volume of condensed liquid. The volume of liquid was obtained by assuming that the condensed phase in the pores had the same density as the bulk liquid, at the temperature of the isotherm. It was found that the total, following summing the ultimate condensed volumes of liquid for the water adsorption isotherm and the nitrogen adsorption isotherm obtained after water adsorption, was equal to the ultimate condensed volume of liquid for the nitrogen adsorption isotherm obtained before water adsorption. This suggests no water escaped the sample between the end of the water adsorption experiment and the start of the second nitrogen adsorption experiment. Figure 4 shows a direct comparison of the water adsorption isotherms for fresh catalyst and coked sample C1. It can be seen that coking leads to a reduction in the amount adsorbed.

The nitrogen adsorption isotherms obtained following coking of fresh catalyst, and/or adsorption of water, were corrected such that the amount adsorbed was expressed per unit mass of catalyst only. The incremental amounts adsorbed over each pressure bin in the nitrogen adsorption isotherm obtained for a given sample after coking and/or water adsorption were subtracted from the corresponding values obtained from the nitrogen

adsorption isotherms for the same sample after coking and/or water adsorption. Where the pressure tables for the adsorption isotherms differed slightly, linear interpolation was used to re-align pressure bin ranges. Figure 5 shows the difference in the incremental amounts of nitrogen adsorbed between the isotherms obtained before and after coking. It can be seen that the effects of coking on nitrogen adsorption are predominantly limited to the relative pressure range 0.7-0.8, with virtually no influence above a relative pressure of 0.8.

In the case of the nitrogen adsorption isotherms obtained before and after water adsorption, the differences in incremental amount of nitrogen adsorbed in each pressure bin were summed in order of increasing pressure to obtain a cumulative adsorbed volume difference plot, as shown in Figure 6 for fresh catalyst and coked sample C1. This plot is analogous to a nitrogen adsorption isotherm for the regions of the void space where the nitrogen adsorption is affected by the adsorbed water. From Figure 6, it can be seen that for the fresh sample there is no impact of water ice on the adsorption of nitrogen above a relative pressure of ~0.7. However, for the coked sample C1, the adsorption of nitrogen is affected at relative pressures above ~0.7. The continued rise of the cumulative adsorbed volume difference plot for C1 above a relative pressure of ~0.7 suggests that the adsorption of water up to a relative pressure of ~0.7 has reduced the amount of nitrogen adsorbing at higher relative pressures. It is also noted that adsorption of nitrogen is affected at relative pressures above 0.8, which is the upper limit affected by coking alone (as seen in Figure 5).

Gas uptake kinetics

Studies of the adsorption kinetics, in the Knudsen diffusion regime, were used to determine the adsorption mass transfer coefficient by employing the linear driving force (LDF) equation [18]:

$$M = M_0(1-\exp(-kt)), \quad (1)$$

where M is the mass uptake at time t, M_0 is the mass uptake at infinite time, and k is the mass transfer coefficient. The mass transfer coefficient was determined by analysing the individual mass uptake vs. time data for each relative pressure point in an isotherm. The fitting was done using the non-linear curve fitting program available in Origin 6.1. Following this, the respective LDF mass transfer coefficients were normalised for the slight fluctuations in sample temperature. This allowed plotting the variation in normalised mass transfer coefficient as a function of a measure of the fraction of the pore volume occupied by condensed liquid nitrogen. The fraction of the pore volume occupied by condensed liquid nitrogen was obtained by taking the ratio of the amount condensed at a particular relative pressure to that obtained at the top of the isotherm or at saturation. Accessible porosity can be defined by Eq. (2):

$$\text{Accessible porosity} = \left[1 - \left(\begin{array}{l}(\textit{fraction occupied by coke}) + \\ (\textit{fraction occupied by liquid } N_2)\end{array}\right)\right]\varepsilon_{fresh} \quad (2a)$$

$$\text{Accessible porosity} = \left[1 - \left(\begin{array}{l}\left(\dfrac{TPV_{fresh} - TPV_{C1}}{TPV_{fresh}}\right) + \\ \left(\dfrac{\textit{vol of condensed liquid } N_2}{TPV_{C1}}\right)\end{array}\right)\right]\varepsilon_{fresh} \quad (2b)$$

for nitrogen adsorption before water adsorption, and by Eq. (3):

$$\text{Accessible porosity} = \left[1 - \left(\begin{array}{l}(\textit{fraction occupied by coke}) + \\ (\textit{fraction occupied by } H_2O) + \\ (\textit{fraction occupied by liquid } N_2)_{\textit{aftee } H_2O \textit{ adsorption}}\end{array}\right)\right]\varepsilon_{fresh} \quad (3a)$$

$$\text{Accessible porosity} = \left[1 - \left(\begin{array}{l}\left(\dfrac{TPV_{fresh} - TPV_{C1}}{TPV_{fresh}}\right) + \\ \left(\dfrac{\textit{vol of condensed liquid } N_{2\,\textit{before } H_2O \textit{ adsorption}} - \textit{vol of condensed liquid } N_{2\,\textit{after } H_2O \textit{ adsorption}}}{TPV_{C1\,\textit{before } H_2O \textit{ adsorption}}}\right) + \\ \left(\dfrac{\textit{vol of condensed liquid } N_2}{TPV_{C1}}\right)_{\textit{after } H_2O \textit{ adsorption}}\end{array}\right)\right]\varepsilon_{fresh} \quad (3b)$$

for nitrogen adsorption after water adsorption. In the above equations, TPV_{fresh} is the total pore volume of the fresh catalyst and ε_{fresh} is the porosity of the fresh catalysts and $TPV_{C1 after H_2O\ adsorption}$ is the total pore volume of nitrogen after water adsorption in material C1. For the coked catalyst C1, before water adsorption, the starting porosity is 0.53. On the other hand, after water adsorption and freezing, the starting porosity is 0.33. Where two samples differ in the amount of void space occupied by coke or water ice, the two conditions can be compared by transforming this plot into one where reduced porosity represents the change in porosity due to the adsorption of nitrogen, i.e., difference between the starting porosity and the accessible porosity at each experimental point.

Figure 7 shows a comparison of the plots of normalised mass transfer coefficient against accessible porosity for fresh and coked catalyst C1 samples. The mass transfer coefficients are presented as their ratio to the highest value obtained for the fresh sample. It can be seen that the normalised *k* values for the fresh sample are initially higher than those for the coked sample, at low nitrogen content.

DISCUSSION

It has been seen that the adsorption of nitrogen above a relative pressure of ~0.7 (the ultimate relative pressure of water) is unaffected by the presence of pre-adsorbed water within the fresh catalyst sample. It is noted that, for adsorption of nitrogen at 77K and water at 298 K, the values of molar density and surface tension etc. are such that the constant of proportionality, between the logarithm of the relative pressure and the reciprocal pore size, in the Kelvin equation is ~1 for both gases. Hence, in a parallel pore bundle pore structure, both nitrogen and water should condense in any given pore size at the same relative pressure.

However, for the coked sample C1, adsorption of nitrogen continues to be affected by pre-adsorbed water up to relative pressures of 0.9, which includes relative pressures above where

nitrogen adsorption is affected by coking alone. The pre-adsorption of water vapour to a relative pressure of ~0.7 in the coked sample leads to a decrease in the amount of nitrogen adsorbed at higher relative pressures than this value. These findings are consistent with the following interpretation. It is supposed that coke lay-down within the fresh catalyst led to a decrease in some larger pore body sizes such that adsorption of water in narrower, neighbouring necks, at relative pressures below 0.7, facilitated filling of these larger pore bodies with water via advanced condensation at that same pressure. In the fresh sample, the equivalent, non-coked pore bodies required water relative pressures higher than 0.7 to fill by condensation, and thus remained unfilled with water. In the nitrogen adsorption experiment following water adsorption, while the larger pore bodies remained empty, and could be filled with nitrogen, for the fresh sample, in the coked sample the larger pore bodies were inaccessible, thereby leading to a drop in nitrogen adsorption even at relative pressures above ~0.7. This interpretation requires that the aforementioned pore bodies and pore necks in the coked sample C1 fill independently for nitrogen but not for water. As has been shown in past simulations [14], the critical ratio of pore body to pore neck size to permit the onset of advanced adsorption depends upon the properties of the fluid, and fluid-surface interaction strength, and is not fixed at a value of 2, as inferred from the Kelvin equation. Previous studies [21] of coking on HDS catalysts have suggested that the coke formed can be highly polar in nature, suggesting that the coke formed here might interact more strongly with water than nitrogen. Hence, the critical pore size ratio for advanced adsorption can be different for nitrogen and water, and lead to differences in the amounts and order of pore-filling as relative pressure is increased. In summary, the above findings suggest that if a standard interpretation of the water adsorption isotherms, employing the assumption of thermodynamically-independent pores, were made, then it would over-estimate the volume of smaller pores filling below a relative pressure of ~0.7 following coking. The pores that become filled with coke would thus seem much smaller than they actually were.

The changes in the mass transfer coefficient following coking can be used to infer some general information regarding coking location. Since the coking of the fresh catalyst to obtain sample C1 leads to a decrease in the mass transfer coefficient this suggests that coking has led to a decrease in the intra-pellet diffusivity. This finding suggests that coke is being deposited nearer the outside of the pellet, rather than towards the centre, which, conversely,

would have led to an increase in the observed value of *k*, due to a decrease in the diffusion path-length [18].

CONCLUSIONS

It has been shown that interpretation of gas adsorption data for coked catalyst must be refined in the light of the advanced adsorption effect. Serial adsorption experiments have shown that this effect is significant, and would lead to erroneous conclusions about the particular pattern of pore structure evolution occurring during coking.

REFERENCES

1. E.S. Kikkinides, A.A. Lappas, A. Nalbadian, I.A. Vasalos, Chem. Engng Sci. 57 (2002) 1011-1025.

2. M. Baghalha, M. Mohammadi, A. Ghorbanpour, Fuel Proc. Tech. 91 (2010) 714-722.

3. D. Chen, H.P. Rebo, A. Holmen, Chem. Engng Sci. 54 (1999) 3465-3473.

4. J. Wood, L.F. Gladden, Appl. Catal. A 249 (2003) 241-253.

5. M. Menéndez, A. Braña, Can. J. Chem. Engng 72 (1994) 926-928.

6. E.P. Barrett, L.G. Joyner, P.H. Halenda, J.Am.Chem.Soc. 73 (1951) 373-380.

7. A.V. Neimark, P.I. Ravikovitch, Micropor. Mesopor. Mat., 44-45 (2001) 697-707.

8. J.H. De Boer, in D.H. Everett, F.S. Stone, (Eds.), The structure and properties of porous solids, Butterworths Scientific Publications: London, 1958; p. 68.

9. L.H. Cohan, J. Am. Chem. Soc., 60 (1938) 433.

10. B. Coasne, A. Galarneau, F. Di Renzo, R.M. Pellenq, J. Phys. Chem. C 111 (2007) 15759-15770.

11. Bruschi, L.; Mistura, G.; Liu, L.; Lee, W.; Gösele, U.; Coasne, B. Langmuir 2010, 26, 11894-11898.

12. F. Casanova, C.E. Chiang, C.-P. Li, I.K. Schuller, Appl. Phys. Lett. 91 (2007) 243103.

13. I. Hitchcock, J.A. Chudek, E.M. Holt, J.P. Lowe, S.P. Rigby, Langmuir 26 (2010) 18061-18070.

14. S.P. Rigby, P. Chigada, Adsorption 15 (2009) 31-41.

15. B. Smarsly, C. Goltner, M. Antonietti, W.Ruland, E. Hoinkis, J. Phys. Chem. B 105 (2001) 831-840.

16. F. Giacobbe, L.A.G. Aylmore, W.A. Steele, J. Colloid Interface Sci. 38 (1972) 277-284.

17. K. Morishige, Y. Kanzaki , J. Phys. Chem. C 113 (2009) 14927-14934.

18. L.-M. Chua, T. Vazhnova, T.J. Mays, D.B. Lukyanov, S.P. Rigby, J.Catal. 271 (2010) 401-412.

19. F. Rouquerol, J. Rouquerol, and K. Sing, Adsorption by Powders and Porous Solids: Principles, Methodology and Applications, Academic Press, London, 1999.

20. A. Shah, R.P. Fishwick, G.A. Leeke, J. Wood, S.P. Rigby, M. Greaves, J. Can. Pet. Tech. 50 (2011) 33-47.

21. C.E. Snape, B.J. McGhee, J.M. Andresen, R. Hughes, C.L. Koon, G. Hutchings, Appl. Catal. A 129 (1995) 125-132.

FIGURE CAPTIONS

Figure 1.

Mercury intrusion and retraction curves for fresh catalyst sample A.

Figure 2.

Nitrogen adsorption isotherms obtained before and after water adsorption, and the intermediate water adsorption isotherm, for a fresh sample, with the amount adsorbed, in each case, expressed as the volume of condensed liquid.

Figure 3.

Nitrogen adsorption isotherms obtained before and after water adsorption, and the intermediate water adsorption isotherm, for the coked sample C1, with the amount adsorbed, in each case, expressed as the volume of condensed liquid.

Figure 4.

A direct comparison of the water adsorption isotherms for fresh catalyst and coked sample C1.

Figure 5.

A plot of the difference in the incremental amounts of nitrogen adsorbed between the isotherms obtained before and after coking.

Figure 6.

Cumulative adsorbed volume difference plots for fresh catalyst and coked sample C1.

Figure 7.

A comparison of the plots of normalised mass transfer coefficient against accessible porosity for fresh and coked catalyst C1 samples.

Figure 1.

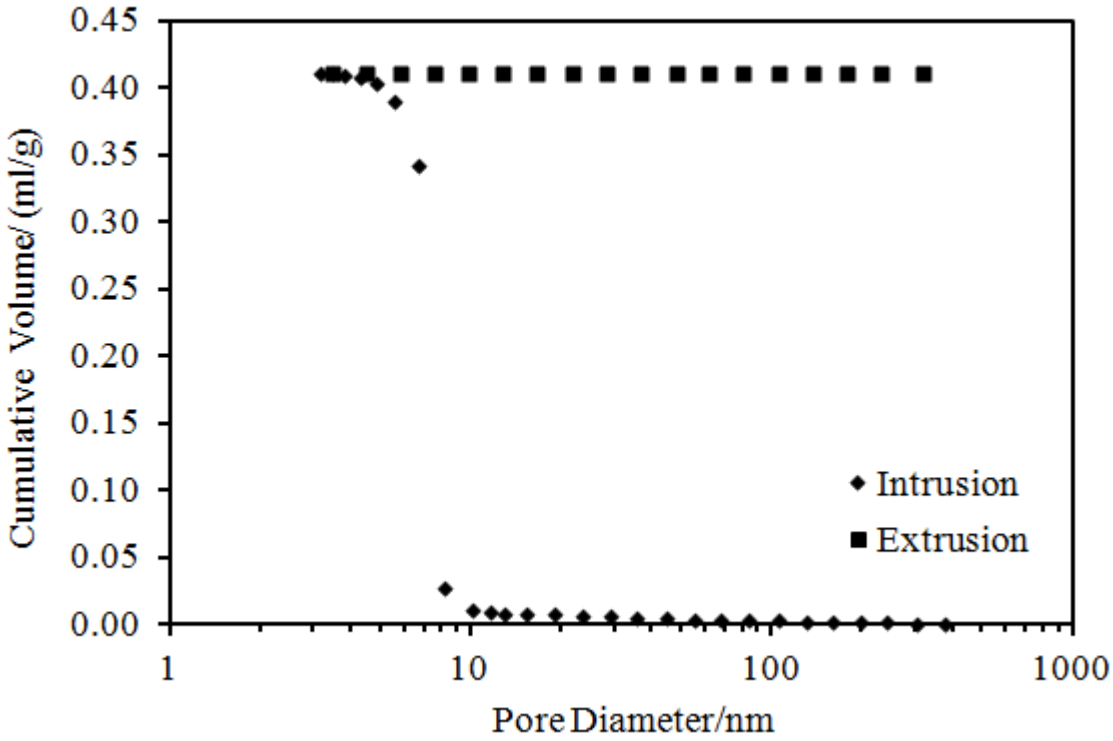
0.45
0.40
0.35
0.30
0.25
0.20
0.15
0.10
0.05
0.00
Cumulative Volume/ (ml/g)
1
10
100
1000
Pore Diameter/nm
Intrusion
Extrusion

Figure 2

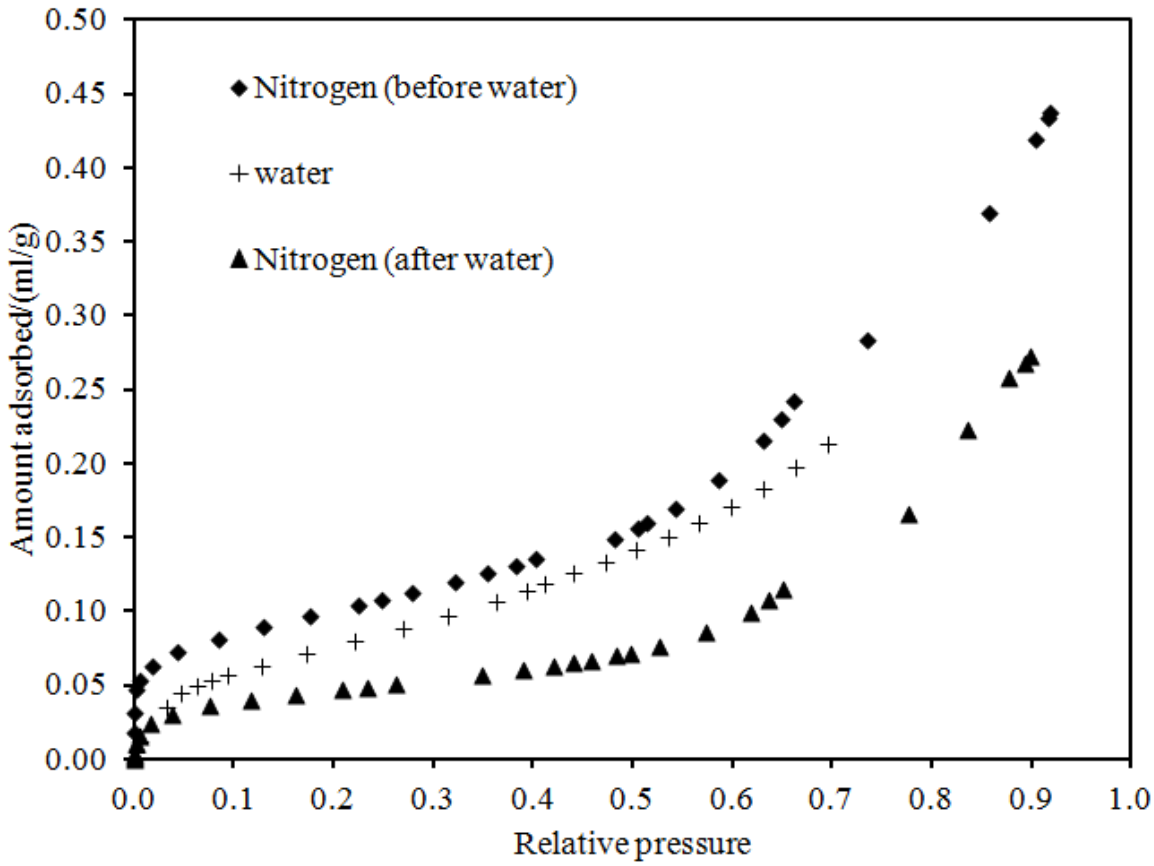
Nitrogen (before water)
water
Nitrogen (after water)
Amount adsorbed/(ml/g)
Relative pressure
0.00
0.05
0.10
0.15
0.20
0.25
0.30
0.35
0.40
0.45
0.50
0.0
0.1
0.2
0.3
0.4
0.5
0.6
0.7
0.8
0.9
1.0

Figure 3

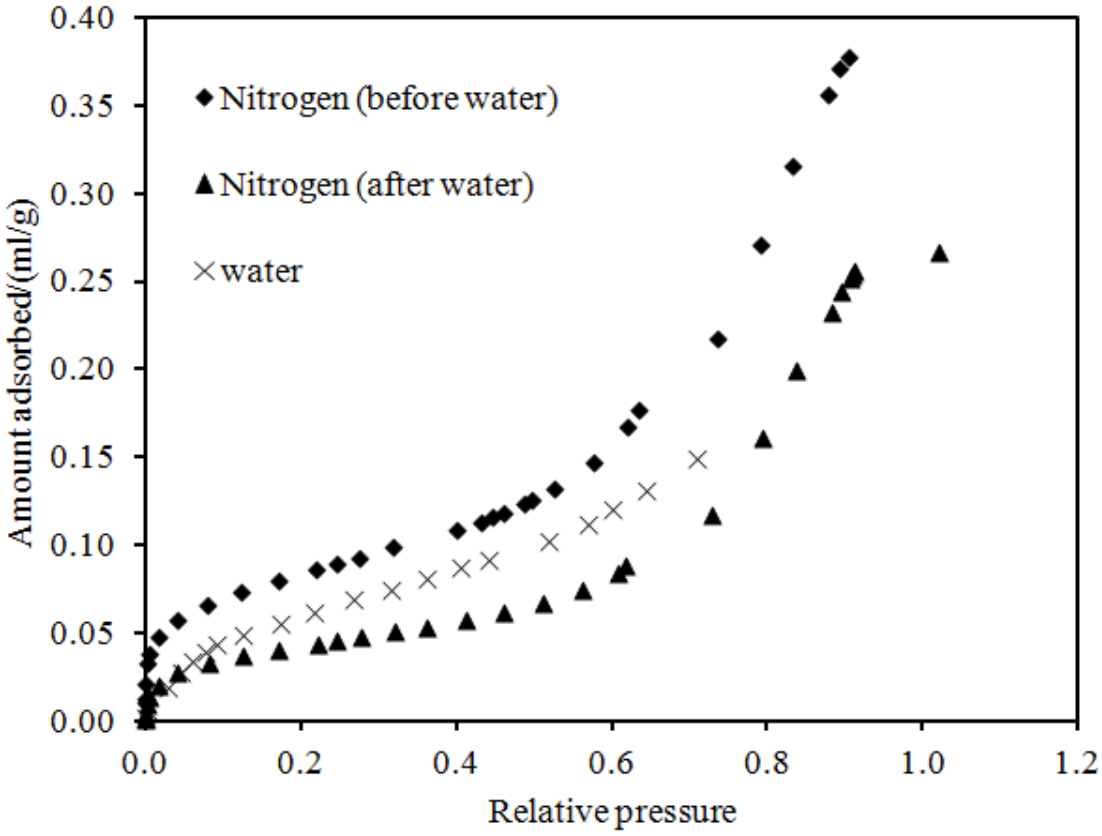
0.40
0.35
0.30
0.25
0.20
0.15
0.10
0.05
0.00
Amount adsorbed/(ml/g)
Nitrogen (before water)
Nitrogen (after water)
water
0.0
0.2
0.4
0.6
0.8
1.0
1.2
Relative pressure

Figure 4

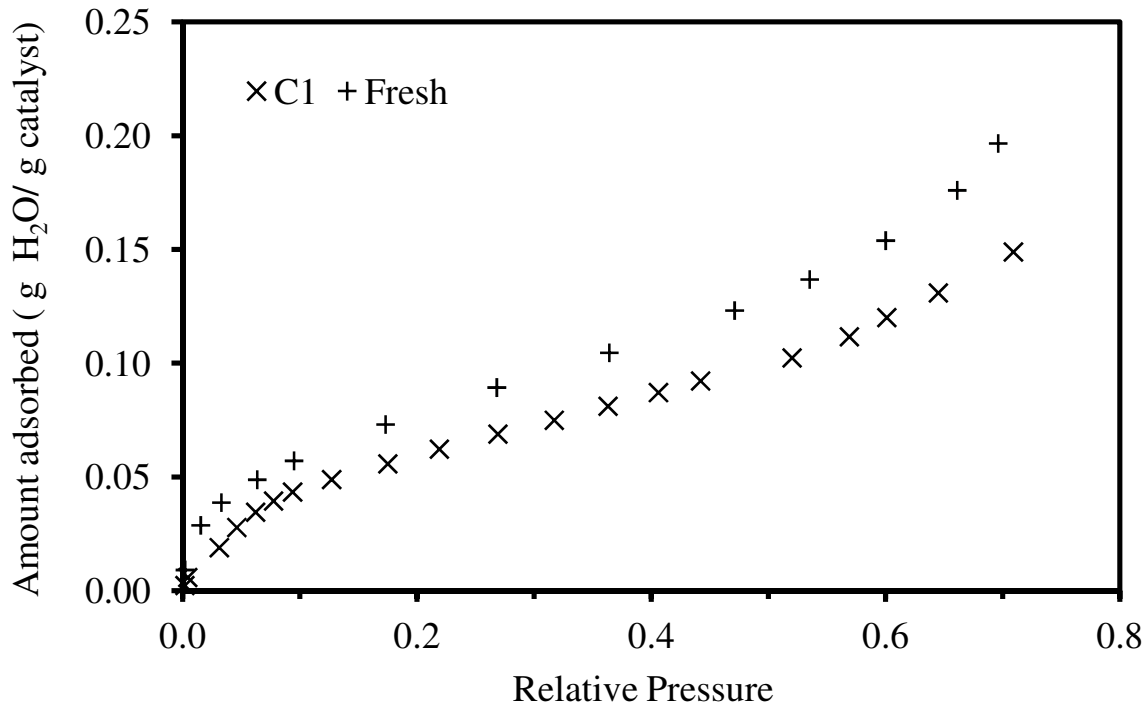
0.25
0.20
0.15
0.10
0.05
0.00
Amount adsorbed (g H2O/ g catalyst)
C1
Fresh
0.0
0.2
0.4
0.6
0.8
Relative Pressure

Figure 5.

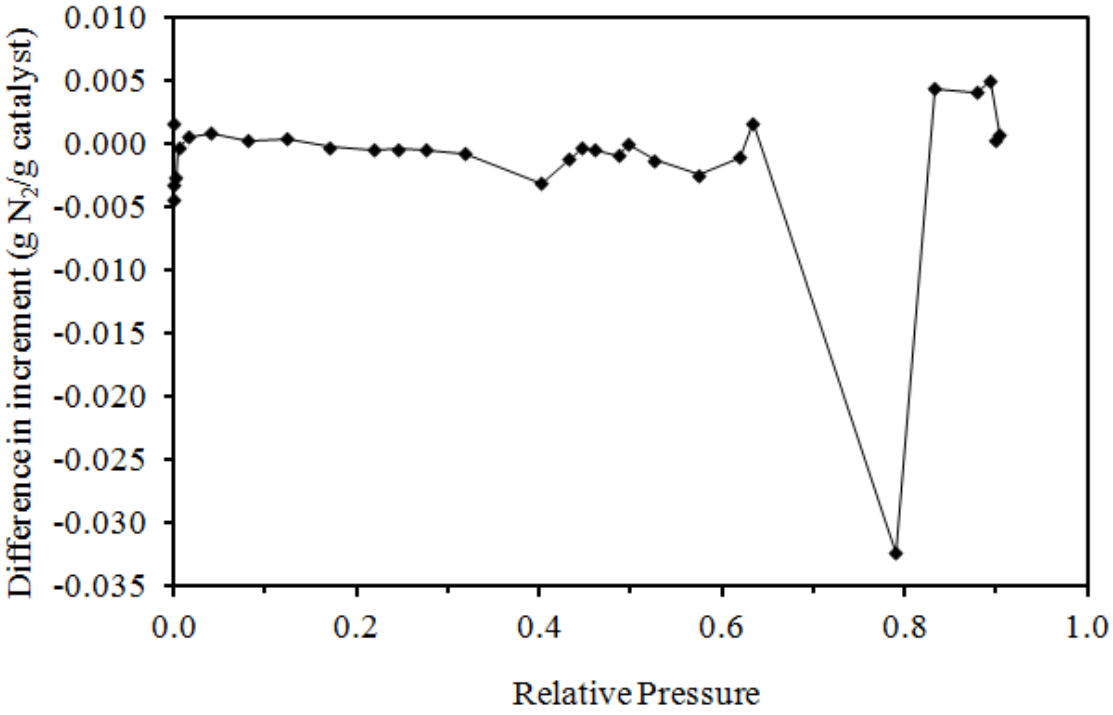
0.010
0.005
0.000
-0.005
-0.010
-0.015
-0.020
-0.025
-0.030
-0.035
Difference in increment (g N2/g catalyst)
0.0
0.2
0.4
0.6
0.8
1.0
Relative Pressure

Figure 6.

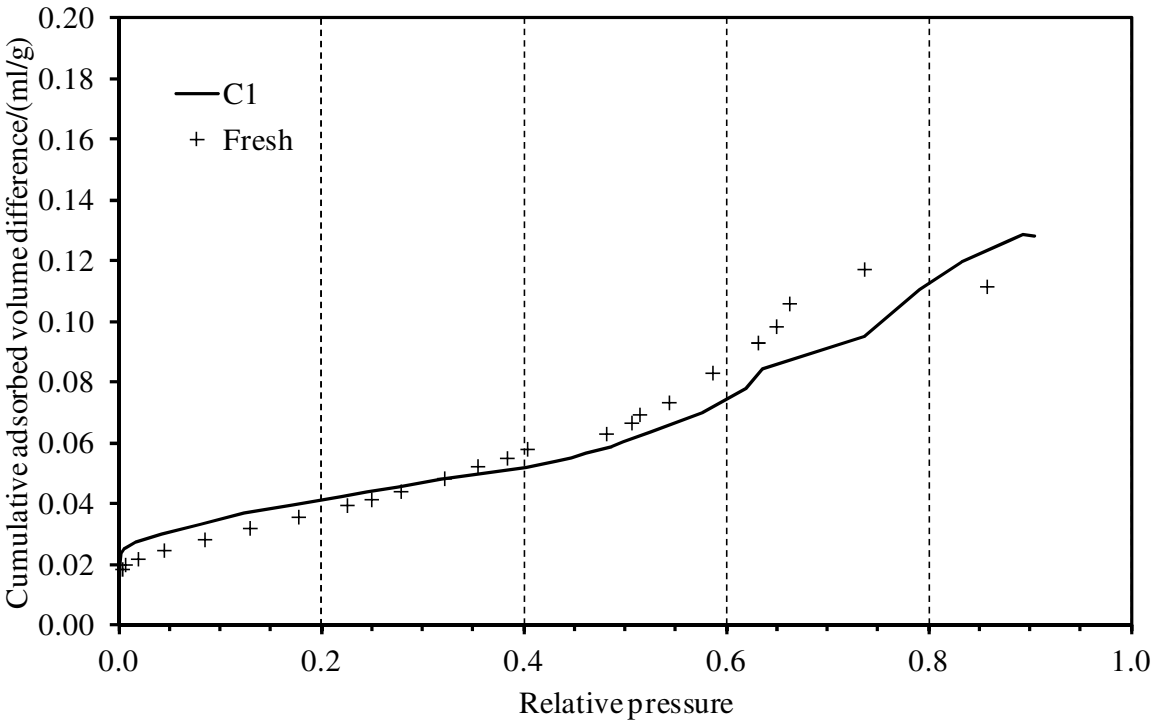
0.20
0.18
0.16
0.14
0.12
0.10
0.08
0.06
0.04
0.02
0.00
Cumulative adsorbed volume difference/(ml/g)
C1
Fresh
0.0
0.2
0.4
0.6
0.8
1.0
Relative pressure

Figure 7.

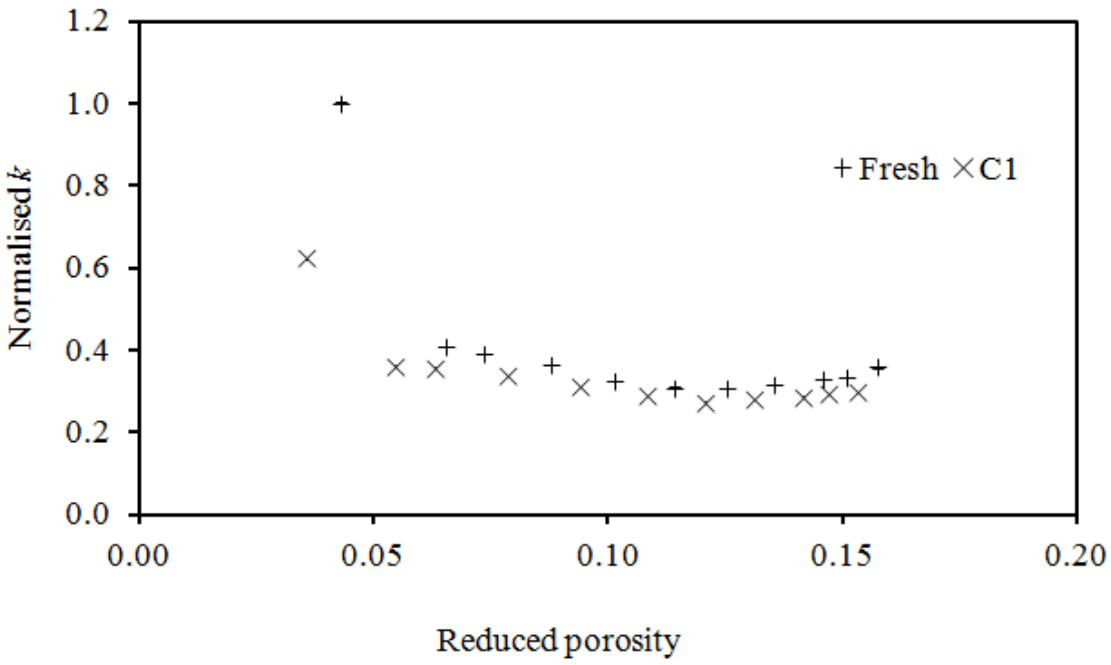
1.2
1.0
0.8
0.6
0.4
0.2
0.0
Normalised k
0.00
0.05
0.10
0.15
0.20
Reduced porosity
+ Fresh × C1